Desmin mediates TNF-α–induced aggregate formation and intercalated disk reorganization in heart failure

Panagiota Panagopoulou,[1] Constantinos H. Davos,[2] Derek J. Milner,[3,4] Emily Varela,[2] JoAnn Cameron,[3,4] Douglas L. Mann,[5] and Yassemi Capetanaki[1]

[1]Cell Biology Division, Center of Basic Research, and [2]Cardiovascular Research Division, Center of Clinical Research, Biomedical Research Foundation, Academy of Athens, Athens 11527, Greece
[3]Department of Cell and Developmental Biology and [4]College of Medicine, Institute for Genomic Biology, University of Illinois at Urbana-Champaign, Urbana, IL 61801
[5]Winters Center for Heart Failure Research, Baylor College of Medicine, Houston, TX 77030

We explored the involvement of the muscle-specific intermediate filament protein desmin in the model of tumor necrosis factor α (TNF-α)–induced cardiomyopathy. We demonstrate that in mice overexpressing TNF-α in the heart (α–myosin heavy chain promoter-driven secretable TNF-α [MHCsTNF]), desmin is modified, loses its intercalated disk (ID) localization, and forms aggregates that colocalize with heat shock protein 25 and ubiquitin. Additionally, other ID proteins such as desmoplakin and β-catenin show similar localization changes in a desmin-dependent fashion. To address underlying mechanisms, we examined whether desmin is a substrate for caspase-6 in vivo as well as the implications of desmin cleavage in MHCsTNF mice. We generated transgenic mice with cardiac-restricted expression of a desmin mutant (D263E) and proved that it is resistant to caspase cleavage in the MHCsTNF myocardium. The aggregates are diminished in these mice, and D263E desmin, desmoplakin, and β-catenin largely retain their proper ID localization. Importantly, D263E desmin expression attenuated cardiomyocyte apoptosis, prevented left ventricular wall thinning, and improved the function of MHCsTNF hearts.

Introduction

TNF-α is a proinflammatory cytokine that has been implicated in the pathogenesis of heart failure. Although the normal heart does not express TNF-α, this cytokine is expressed within the myocardium as well as in the peripheral circulation in patients with heart failure (Latini et al., 1994; Torre-Amione et al., 1996). When selectively overexpressed in the mouse heart, TNF-α leads to the development of a dilated cardiomyopathy (DCM) that recapitulates the classical transition to failure with progressive left ventricle (LV) dysfunction and remodeling, cardiac myocyte hypertrophy, interstitial fibrosis, and progressive myocyte loss by apoptosis (for reviews see Feldman et al., 2000; Mann, 2003). Recently, we have shown that TNF-α provokes cardiomyocyte apoptosis and LV wall thinning through activation of both the extrinsic and the intrinsic apoptotic pathways that converge on effector caspases (Haudek et al., 2007).

Active effector caspases cleave several intracellular substrates, including various cytoskeletal components, leading to cytoplasmic budding, nuclear condensation, and formation of apoptotic bodies (Kayalar et al., 1996; Caulin et al., 1997). The reorganization of intermediate filaments (IFs) seems to be a main target during apoptosis because many structurally related IF proteins are specifically cleaved by different members of the caspase family within the L1–L2 linker region between two conserved α-helical domains. The first IF proteins identified as caspase substrates were the nuclear lamins (Lazebnik et al., 1995) followed by the cytoplasmic IF proteins, cytokeratins 14, 18, and 19, vimentin, and desmin (Caulin et al., 1997; Ku et al., 1997; Byun et al., 2001; Chen et al., 2003). However, the biological significance of this caspase action on IFs is presently unknown.

In adult cardiomyocytes, desmin, the muscle-specific IF protein, forms a 3D scaffold that links the contractile apparatus to the costameres of plasma membrane, intercalated disks (IDs), the nucleus, and also other membranous cellular organelles (for

C.H. Davos, D.J. Milner, and E. Varela contributed equally to this paper.

Correspondence to Yassemi Capetanaki: ycapetanaki@bioacademy.gr

Abbreviations used in this paper: DCM, dilated cardiomyopathy; DRM, desmin-related myopathy; EDD, end diastolic diameter; FS, fractional shortening; HSP, heat shock protein; ID, intercalated disk; IF, intermediate filament; LV, left ventricle; PWT, posterior wall thickness; UPS, ubiquitin proteasome system; WT, wild type.

The online version of this article contains supplemental material.

The Rockefeller University Press $30.00
J. Cell Biol. Vol. 181 No. 5 761–775
www.jcb.org/cgi/doi/10.1083/jcb.200710049

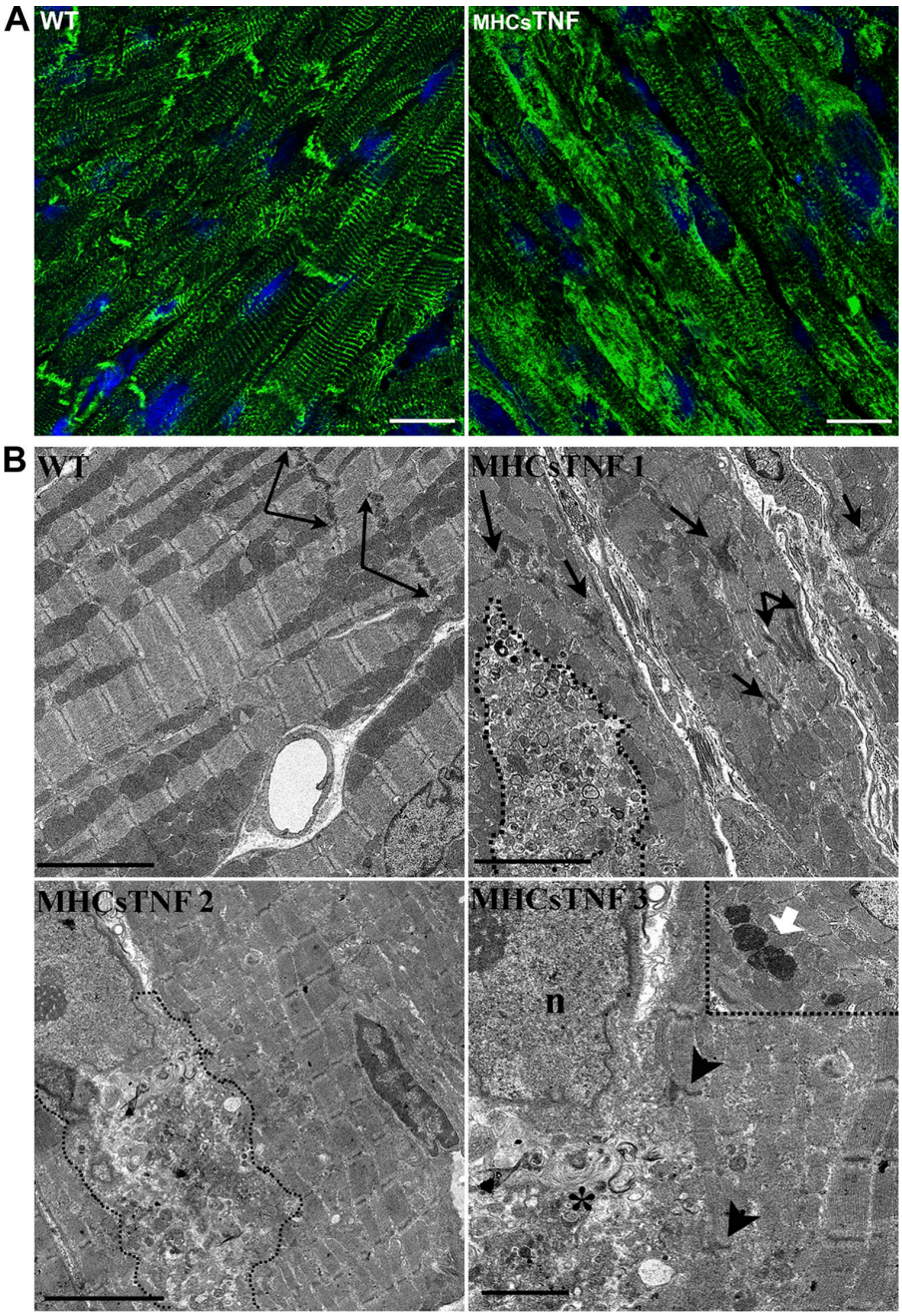

Figure 1. **Desmin is absent from IDs and forms cytoplasmic aggregates in MHCsTNF mice.** (A) Representative myocardial cryosections from 3-mo-old WT and MHCsTNF littermates were labeled for desmin and analyzed by confocal microscopy. Nuclei were stained with DAPI. (B) Electron micrographs from 3-mo-old WT and MHCsTNF mice. Arrows in WT point to IDs. Perinuclear aggregates and sarcoplasmic aggregates are displayed in TNF 2 and 1, respectively. Aggregates are outlined with dashed lines. TNF 3 is an enlargement of TNF 2 showing Z disks adjacent to an aggregate (asterisk) with material apparently merging into the aggregate (arrowheads). The white arrow in the inset of TNF 3 shows aggregates with electron-dense material. n, nucleus. Bars: (A) 20 µm; (B, top and bottom left) 5 µm; (B, bottom right) 2 µm.

reviews see Capetanaki et al., 1997, 2007). Attempts to determine the function of desmin have increased over recent years, as mutations within its gene have been linked to several human inherited myopathies called desmin-related myopathies (DRMs), which are characterized by desmin-positive amorphous or granular material (Bar et al., 2004; Schroder et al., 2007; for review see Goldfarb et al., 2004). Desmin, together with other cytoskeletal proteins, forms a continuous network that extends from the nuclear to the extracellular matrix (for review see Capetanaki et al., 2007). Human mutations of different components of this network, including desmin, are linked to DCM and heart failure (for review see Seidman and Seidman, 2001; Towbin and Bowles, 2002). Therefore, it has been speculated that in addition to the known DRMs, desmin might be involved indirectly in different cardiomyopathies caused by mutations in other components of the network.

A milestone in our current understanding of desmin function was the generation of desmin-null mice (Li et al., 1996; Milner et al., 1996). Desmin-deficient mice develop a progressive and generalized myopathy that mainly affects the myocardium. In desmin-null mice, transient cardiomyocyte hypertrophy is followed by the development of a DCM that is characterized by mitochondrial ultrastructural and other defects, calcified and fibrotic lesions, and extensive cell death (Li et al., 1996; Milner et al., 1996; Thornell et al., 1997). Desmin has also been implicated in the apoptotic pathway because it is cleaved specifically at the 263 aspartic acid residue (D), by caspase-6 in vitro, as well as in myogenic cells induced to undergo apoptosis after treatment with TNF-α (Chen et al., 2003).

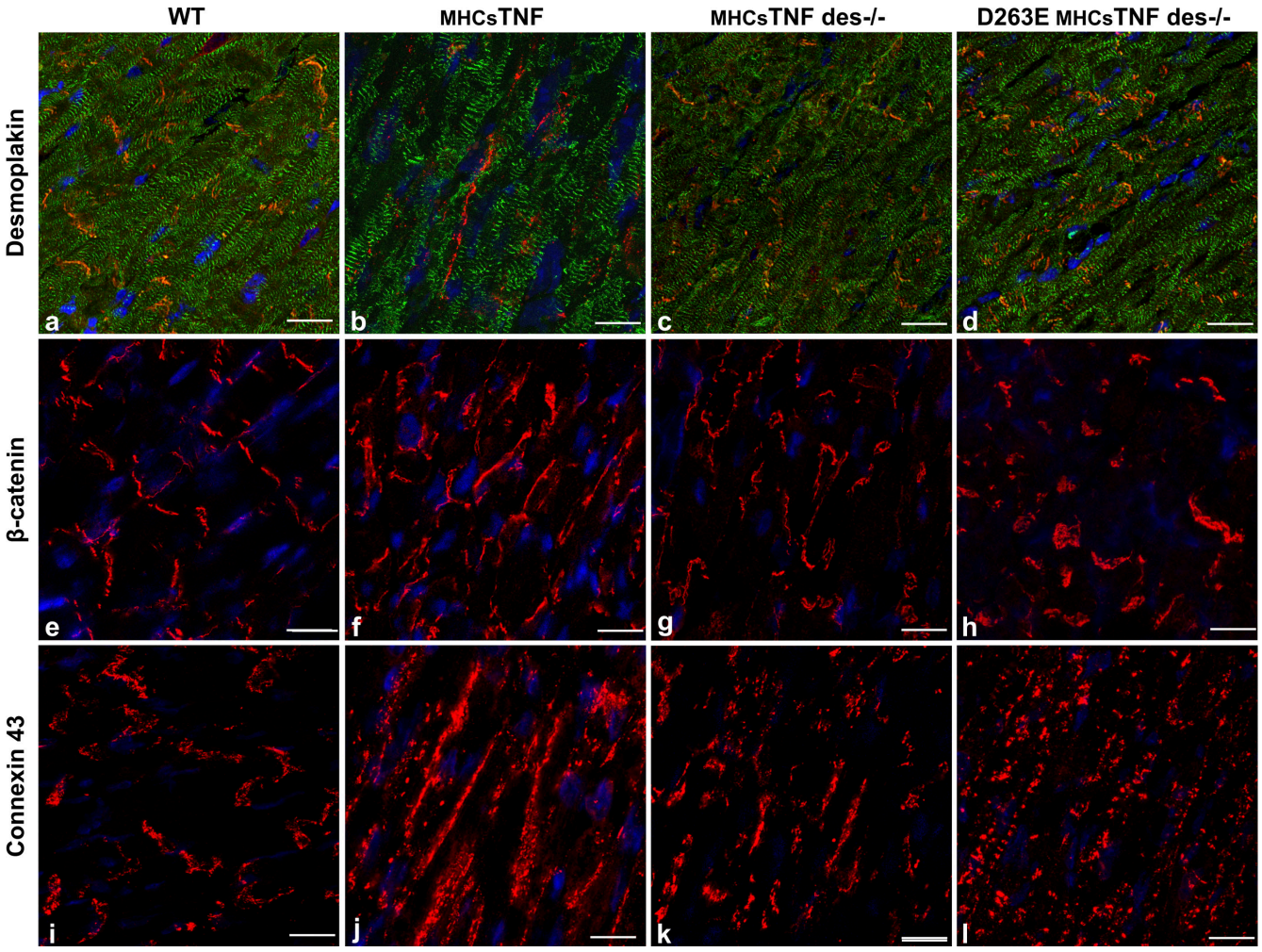

Figure 2. **Desmin is implicated in TNF-α–induced desmoplakin and β-catenin mislocalization.** Myocardial cryosections from WT (a, e, and i), MHCsTNF (b, f, and j), MHCsTNF des$^{-/-}$ (c, g, and k), and D263E MHCsTNF des$^{-/-}$ (d, h, and l) mice at 3 mo of age were labeled for β-catenin (e–h) and connexin 43 (i–l) and were double labeled for α-actinin (green) and desmoplakin (red; a–d) followed by confocal microscopy analysis. Double labeling with α-actinin was done in all cases but is shown only in one (with desmoplakin) just to visualize the orientation of the cells; it is not shown for the rest because its high intensity masks the ID signal. Nuclei were stained with DAPI. Bars, 20 μm.

In an effort to investigate the potential involvement of desmin in the cascade of events leading to TNF-α–induced cardiomyopathy, we examined its intracellular distribution in transgenic mice with cardiac-restricted overexpression of secreted TNF (α–myosin heavy chain promoter-driven secretable TNF-α [MHCsTNF] mice). In this study, we demonstrate that in cardiomyocytes from the MHCsTNF hearts, desmin forms aggregates and is absent from IDs. The recently discovered and defined cardiomyocyte junctional structures, termed area composita (Franke et al., 2006), were also affected in a desmin-dependent fashion. Ultrastructural experiments revealed that the architecture of the IDs is generally affected in MHCsTNF hearts. To assess the importance of desmin's cleavage in vivo, we outcrossed transgenic mice that express only the desmin mutant (D263E), which is resistant to cleavage by caspase-6, with the MHCsTNF mice. These experiments revealed that the TNF-α–induced cleavage of desmin is an important mechanism for its loss from IDs. The products of the desmin cleavage are detected in ubiquitin-positive aggregates, whereas in the TNF-α myocardium expressing the transgenic D263E desmin, a number of these aggregates were decreased and were not colocalized with desmin. Apart from relocation of the ID proteins, the D263E desmin attenuated cardiomyocyte apoptosis, prevented LV wall thinning, and improved the function of the MHCsTNF hearts.

Results

TNF-α overexpression leads to desmin aggregation and disappearance from IDs

Desmin is normally localized at Z disks and IDs of cardiac muscle. Using confocal microscopy, we investigated the potential effect of TNF-α on desmin localization. As shown in Fig. 1 A, TNF-α overexpression leads to desmin aggregation and loss from ID structures but not from Z disks. To study the temporal pattern of this alteration, we looked as early as 15 d after birth and found that desmin was already absent from the IDs (Fig. S1, a and b; available at http://www.jcb.org/cgi/content/full/jcb.200710049/DC1). Aggregate formation and ID abnormalities were confirmed by ultrastructural experiments (Fig. 1 B). As shown in Fig. 1 B, electron micrographs from 3-mo-old MHCsTNF mice revealed the

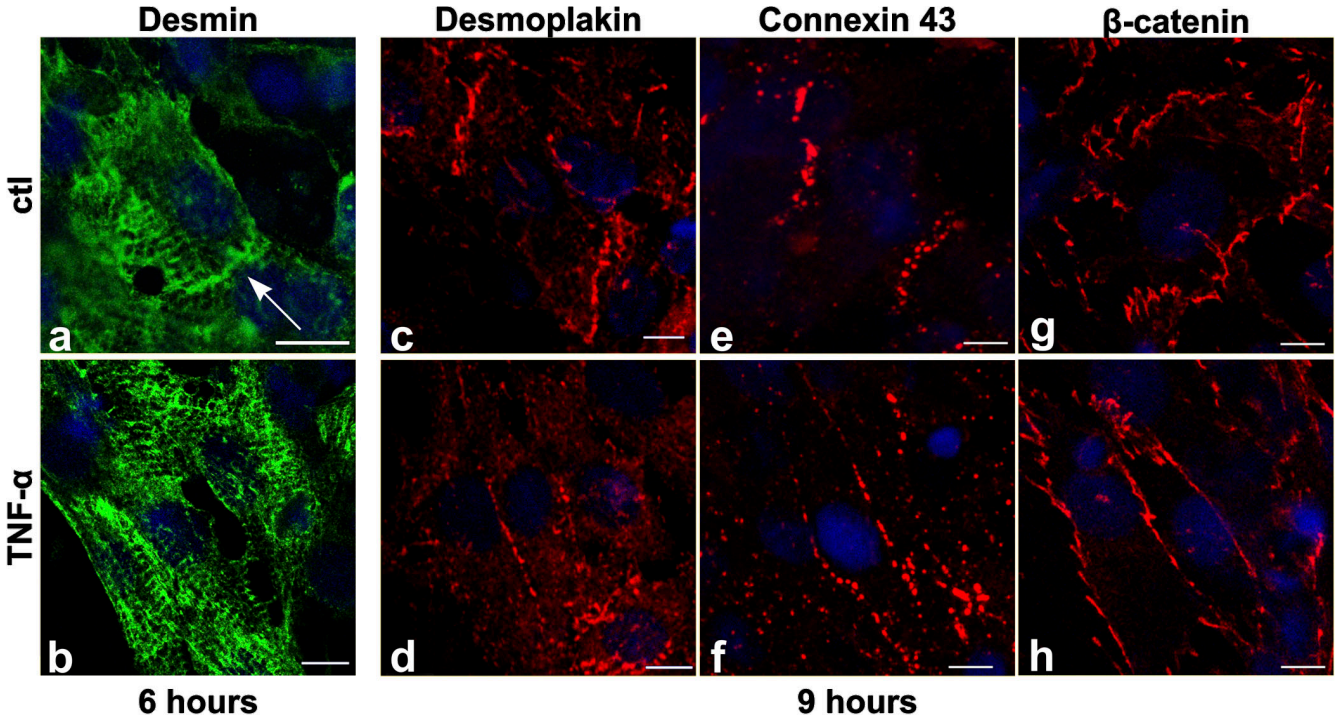

Figure 3. **Addition of TNF-α to in vitro cultured cardiomyocytes induces the withdrawal of desmin, β-catenin, desmoplakin, and connexin 43 from the ID structure.** Neonatal rat cardiomyocytes were incubated with TNF-α for the indicated time periods (b, d, f, and h). Cells were immunostained for desmin (a and b), desmoplakin (c and d), connexin 43 (e and f), and β-catenin (g and h) and analyzed by confocal microscopy. The arrow indicates the presence of desmin at IDs in the control culture. Nuclei were stained with DAPI. Bars, 10 μm.

presence of numerous amorphous aggregates in the sarcoplasm. The aggregates were variable in composition, consisting of differing amounts of granular material, vesicles, membranous whorls, and, occasionally, clumps of electron-dense material (Fig. 1 B, TNF3). Mitochondria were also found scattered throughout some aggregates. These aggregates disrupted the normal alignment of myofibrils and frequently exhibited perinuclear localization.

The IDs in MHCsTNF samples also displayed abnormalities. Unlike the long, steplike IDs frequently observed in normal myocardium, MHCsTNF IDs were more punctuate and disorganized (Fig. 1 B, TNF1). Compared with normal myocardium, IDs were also more sparse and difficult to detect. Z disks displayed abnormalities as well, frequently appearing wavy or bent. Occasionally, material from Z disks adjacent to aggregates appeared to be streaming into the aggregate (Fig. 1 B, TNF3). Mitochondrial shape changes, swelling, and lysis were also observed, as were apoptotic myonuclei. Our studies confirm some previous observations, which had also revealed abnormalities in myofibril alignment as well as mitochondrial defects in MHCsTNF myocardium (Li et al., 2001; Sivasubramanian et al., 2001).

TNF-α overexpression leads to progressive mislocalization of ID proteins in vivo and in vitro

To examine whether the TNF-α–induced malformation of IDs influences the position of the ID proteins, we performed similar immunofluorescent experiments using antibodies against desmoplakin, β-catenin, and connexin 43, which are characteristic proteins of desmosomes, adherent junctions, and gap junctions, respectively. At day 15 after birth, desmoplakin and β-catenin localize almost normally in MHCsTNF mice in contrast to connexin 43, which has already moved from IDs to the lateral side of cardiomyocytes (Fig. S1, c–h). However, in the 3-mo-old MHCsTNF mice, all studied proteins were primarily localized at the lateral, nonjunctional side of the cardiomyocytes (Fig. 2).

Because desmin is absent from IDs from the earliest time point examined (15 d), TNF-α could modify desmin and either provoke its removal from or inhibit its association with IDs. With the goal of eventually distinguishing between inhibition of targeting to the IDs versus modification, destabilization, and removal of desmin from its position in the IDs, we investigated the dynamics of the TNF-α–induced alterations in desmin in vitro in primary culture of neonatal rat cardiomyocytes. 6 h after the addition of TNF-α, desmin completely disappeared from IDs, whereas desmoplakin, β-catenin, and connexin 43 required ∼9 h of TNF-α stimulation for their complete relocalization at the lateral side of cardiomyocytes, with only traces of the proteins detected at the IDs (Fig. 3). These data suggest that desmin is the primary target of TNF-α modification, leading to its removal from IDs accompanied by the subsequent withdrawal of the other ID proteins from there.

TNF-α induces the modification and accumulation of desmin

To address whether TNF-α signaling leads to the posttranslational modification of desmin that might contribute to its removal from IDs, we performed 2D gel electrophoresis of heart crude extracts from wild-type (WT) and MHCsTNF animals followed by Western blot analysis. As shown in Fig. 4 A, desmin was more

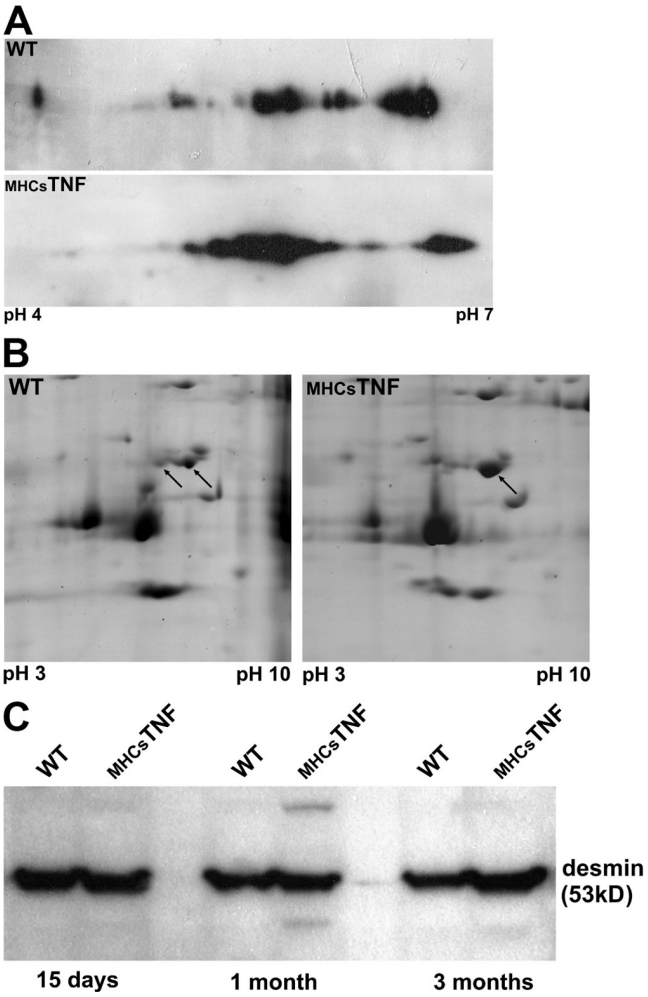

Figure 4. **Accumulation and modification of desmin in the MHCsTNF heart.** (A) Crude extracts from hearts of 3-mo-old WT and MHCsTNF mice were electrophoretically analyzed in the first dimension by using pH 4–7 IPGphor strips and in the second dimension by 12% SDS-PAGE followed by immunoblotting using antibody for desmin. (B) Gels similar to those transferred to polyvinylidene difluoride membranes (IPG-strips pH 3–10) were counterstained with colloidal Coomassie Brilliant blue to visualize the protein loading. The arrows indicate spots identified as desmin by mass spectrophotometry. (C) Representative Western blot showing the protein expression levels of desmin at mice of different ages (15 d and 1 and 3 mo).

abundant and more acidic in MHCsTNF hearts than the corresponding protein in WT hearts. This is most likely the result of higher levels of its phosphorylated isoforms, suggesting that TNF-α posttranslationally modifies desmin, presumably leading to the disassembly of desmin filaments and their removal from IDs.

Desmin quantification in heart crude extracts from 3-mo-old mice revealed an ∼60% increase in the protein level of MHCsTNF hearts compared with WT. The increase of desmin at the protein level does not reflect an increase of desmin mRNA levels as shown by real-time RT-PCR experiments (not depicted), indicating that desmin is accumulating in the cardiomyocytes from MHCsTNF hearts.

TNF-α causes desmin-positive aggregate formation that colocalizes with HSP25

Another important observation of this study is that desmin forms aggregates in the myocardium of MHCsTNF mice. Because cytoplasmic accumulation of small heat shock proteins (HSPs) along with desmin-positive aggregates is an immunohistochemical characteristic of human desminopathies (Fischer et al., 2002), we examined whether desmin colocalizes in these aggregates with the chaperone HSP25. We found that desmin aggregates colocalize with HSP25 (Fig. 5 A). HSP25 exhibits both a cytoplasmic and striated staining pattern in WT longitudinal sections of cardiomyocytes incubated with anti-HSP25 (Fig. 5 A, f). The striated pattern resembles that of desmin, as shown by colocalization experiments (Fig. 5 A). In MHCsTNF myocardium, there are also HSP25 aggregates that do not colocalize with desmin and are located around vessels. Desmin also displays another form of aggregates that colocalize with ubiquitin and tend to distribute close to nuclei, as described in the next paragraph.

As protein aggregates are insoluble in extraction buffer that contain nonionic detergents such as Triton X-100, we performed Western blot analysis for HSP25 of both the Triton-X insoluble fraction (associated with the aggregates) and the soluble fraction (cytoplasmic) of proteins isolated from 3-mo-old WT and MHCsTNF mouse hearts. HSP25 was increased in both fractions in MHCsTNF hearts as shown in Fig. 5 B. Phosphorylation is the major posttranslational modification of HSP25 in response to multiple forms of cellular stress (Fischer et al., 2002). To address whether TNF-α induces a posttranslational modification in HSP25, we examined its pattern in 2D gel electrophoresis. In TNF-α–overexpressing hearts, HSP25 demonstrated an increase in one of the acidic isoforms when compared with the WT (Fig. 5 C). Interestingly, there was also an additional, more alkaline isoform (Fig. 5 C) identified in the MHCsTNF mouse heart that was completely absent from WT and is known to be correlated with desminopathies (Clemen et al., 2005).

The absence of desmin from hearts that overexpress TNF-α attenuates the mislocalization of ID proteins and reduces HSP25 aggregation

To investigate the importance of desmin in the TNF-α–induced loss of ID protein localization, we studied their distribution in desmin-null ($des^{-/-}$) mice. The absence of desmin induces changes in the architecture of IDs with characteristic increased intraplaque space, as has been demonstrated by electron microscopy studies (Capetanaki et al., 1997; Thornell et al., 1997). Examination of the localization of these three proteins in the $des^{-/-}$ myocardium revealed that their proper localization at the IDs is desmin independent (Fig. S2, b, e, and h; available at http://www.jcb.org/cgi/content/full/jcb.200710049/DC1).

When we crossed MHCsTNF mice with $des^{-/-}$ mice and studied the MHCsTNF $des^{-/-}$ hearts, we found that in the absence of desmin, both desmoplakin and β-catenin retained their ID localization at high degree (Fig. 2, c and g). On the other hand, the localization of connexin 43 was not restored in the MHCsTNF $des^{-/-}$ hearts, as depicted in Fig. 2 k. Therefore, the observed alterations in desmoplakin and β-catenin localization in the MHCsTNF mouse hearts are desmin dependent because the absence of desmin largely attenuates the subcellular relocalization of these proteins of the area composita. In contrast, the altered pattern of connexin 43 seems to be regulated by TNF-α in a desmin-independent manner.

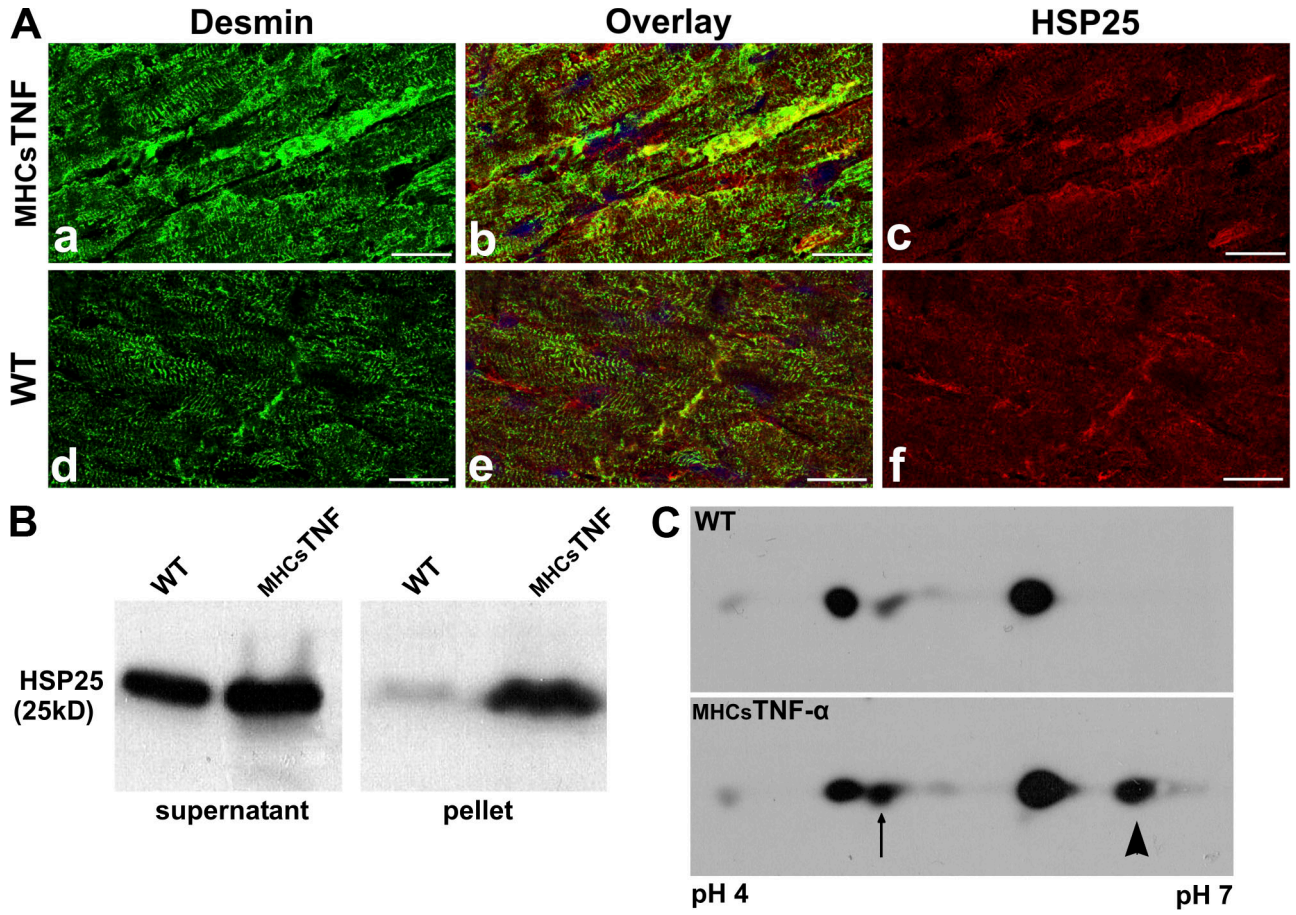

Figure 5. **HSP25 is modified and colocalizes with desmin in subcellular aggregates of the MHCsTNF myocardium.** (A) Immunofluorescent data from ventricular cryosections of 3-mo-old WT (d–f) and MHCsTNF (a–c) littermates were double labeled for desmin (a and d; green) and HSP25 (c and f; red) and analyzed by confocal microscopy. Nuclei were stained with DAPI. (B) Protein expression levels of HSP25 in 3-mo-old WT and MHCsTNF mice. (C) Western blot analysis of HSP25 from 2D gel electrophoresis of hearts from WT and MHCsTNF mice. Total protein extracts were electrophoretically analyzed in the first dimension by using pH 4–7 IPGphor strips and in the second dimension by 12% SDS-PAGE followed by immunoblotting analysis using antibody for murine HSP25. The arrow indicates the acidic isovariant that is increased in the MHCsTNF myocardium, and the arrowhead shows the alkaline isovariant that is present only in the sample from the MHCsTNF heart. Bars, 20 μm.

To determine the role of desmin in the TNF-α–induced aggregation of HSP25, we examined the subcellular distribution of HSP25 in the myocardium of MHCsTNF des$^{-/-}$ mice. Immunofluorescent experiments revealed that HSP25 aggregates were considerably decreased and restricted only to perivascular areas (not depicted). We did not observe any cytoplasmic aggregates of HSP25, indicating that modified desmin was responsible for HSP25 accumulation in cardiomyocytes, whereas the absence of desmin did not lead to HSP25 aggregation. Interestingly, the amorphous aggregates seen in MHCsTNF cardiomyocytes at the ultrastructural level are absent in MHCsTNF des$^{-/-}$ mice (not depicted).

The TNF-α–induced caspase cleavage of desmin mediates its removal from IDs and the mislocalization of desmoplakin and β-catenin

Transgenic expression of D263E, a caspase-resistant desmin, rescues the phenotype of des$^{-/-}$ mice. Desmin is cleaved specifically by caspase-6 at VEMD↓M^{264} in its L1–L2 linker domain in vitro (Chen et al., 2003). We have previously shown that TNF-α activates caspase-dependent apoptotic cell death pathways (Haudek et al., 2007). To test the hypothesis that desmin cleavage is involved in its removal from IDs in the MHCsTNF mouse hearts, we generated transgenic mice that express a desmin mutant (D263E) harboring a substitution of the 263 aspartic acid (D) with a glutamic acid (E), which renders desmin resistant to caspase-mediated cleavage. Three mouse lines were generated using the αMHC promoter to target the expression of desmin D263E to cardiomyocytes (lines 66, 74, and 91).

Southern blot analysis of genomic DNA from the three lines revealed differences in the copy number of the transgene (Fig. 6 A). However, Western blot analysis from whole heart extracts indicates that at the protein level, desmin in line 66 was similar to that of WT levels, whereas it is at a higher level than WT in lines 74 and 91 (Fig. 6 B). The aforementioned three lines were bred with des$^{-/-}$ mice over two generations to produce mice null for endogenous desmin but harboring the D263E transgenic desmin (D263E des$^{-/-}$). Although des$^{-/-}$ hearts displayed the expected defects, including large areas of calcium deposits at the external surface of the heart and extensive fibrotic lesions, as shown by the histological analysis

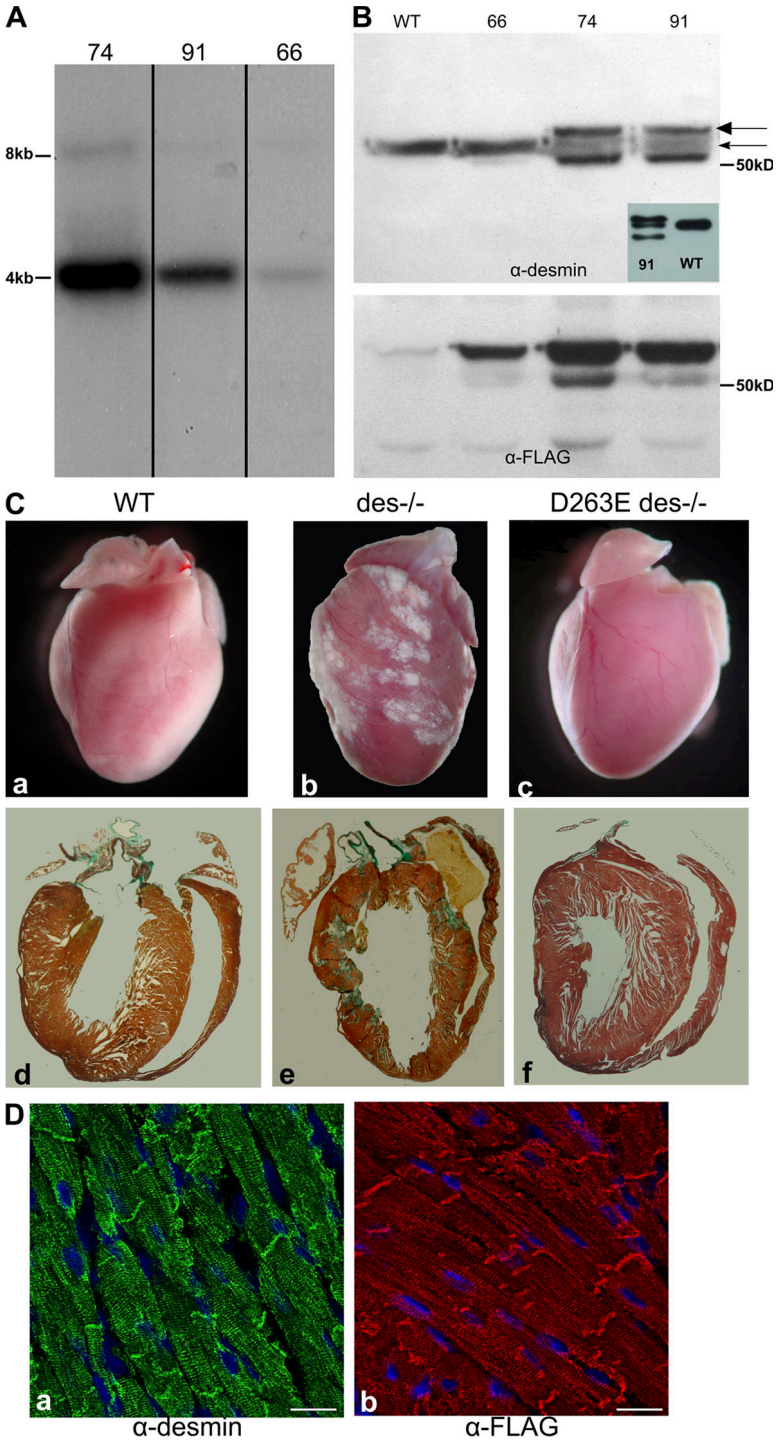

Figure 6. **D263E transgenic desmin rescues the des$^{-/-}$ phenotype.** Morphological and histological analysis. (A) Southern blot analysis from genomic DNA of the three different lines generated (66, 74, and 91), revealing the difference in transgene copy number. (B) Desmin protein expression in the three lines. Heart homogenates were analyzed in 10% SDS-PAGE and immunoblotted using anti-Flag and anti-desmin antibodies. The thin arrow indicates the endogenous desmin, and the thick arrow shows the Flag-tagged desmin. Hearts from line 66 express mainly the endogenous desmin, but overexposure of the film shows that the mutant D263E desmin is expressed at low levels (not depicted); this is also confirmed by the α-Flag. The bottom band is most possibly a desmin degradation product that is always visible at high desmin concentrations. The consistency of this band has been verified with other desmin antibodies, which are shown in the inset. (C) Gross morphology of hearts (top) and masson-stained paraffin sections (bottom) from 3-mo-old WT (a and d), des$^{-/-}$ (b and e), and D263E des$^{-/-}$ (c and f) animals. (D) Representative myocardial cryosections from D263E des$^{-/-}$ mice were labeled for desmin (a) and desmin-Flag (b) and analyzed using confocal microscopy. Bars, 20 μm.

(Fig. 6 C), D263E des$^{-/-}$ hearts from 3-mo-old littermates appeared identical to WT. Thus, cardiomyocyte-specific expression of D263E desmin is capable of rescuing the gross morphology of the des$^{-/-}$ heart. Examination of the subcellular localization of D263E desmin in sections from D263E des$^{-/-}$ mice showed a staining pattern identical to that of WT (Fig. 6 D). In all of the transgenic lines we examined (66, 74, and 91), we did not detect desmin-enriched inclusion bodies or other abnormalities in cardiac sections. Similarly, desmoplakin, β-catenin, and connexin 43 displayed a normal distribution at IDs (Fig. S2, c, f, and i).

D263E desmin is resistant to TNF-α–induced caspase cleavage and partially restores the proper localization of desmin and other proteins at the IDs. To determine whether desmin is specifically cleaved in vivo by TNF-α–induced caspases, at the expected site, we generated bitransgenic (D263E MHCsTNF des$^{-/-}$) mice expressing only the D263E desmin by crossing D263E des$^{-/-}$ with MHCsTNF des$^{-/-}$ mice. As shown in Fig. 7 A, Western blot analysis revealed that the expected desmin caspase fragments (24 and 29 kD) were only detected in tissue homogenates from

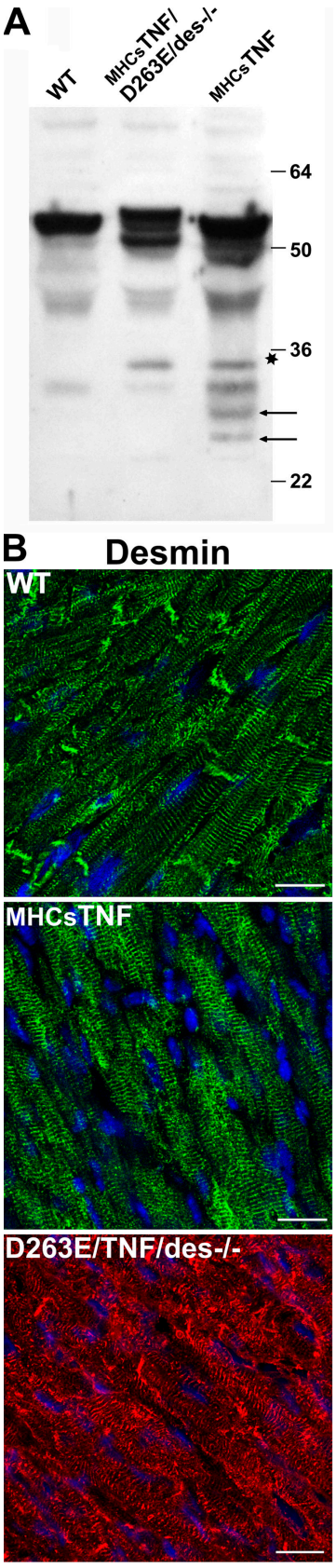

Figure 7. **TNF-α–induced desmin cleavage is responsible for its relocalization away from the IDs.** (A) Heart homogenates from WT, MHCsTNF, and D263E MHCsTNF des$^{-/-}$ mice were analyzed in 12% SDS-PAGE and immunoblotted with polyclonal antibody recognizing the entire desmin molecule. The arrows indicate the two TNF-α–induced caspase cleavage desmin fragments present only in TNF-α hearts. The asterisk shows a band that seems to be a TNF-α–related degradation product absent from WT. The other bands, which are common to the three specimens, are general desmin degradation products. (B) Representative myocardial cryosections from 3-mo-old WT, MHCsTNF, and D263E MHCsTNF des$^{-/-}$ mice were labeled for desmin and analyzed using confocal microscopy. Bars, 20 μm.

MHCsTNF mice and were absent from extracts of both WT and bitransgenic mice. To determine the functional significance of desmin cleavage in vivo, we examined its subcellular localization in D263E MHCsTNF des$^{-/-}$ mice. As shown in Fig. 7 B, desmin was localized primarily at the IDs. Furthermore, the other proteins of the area composita, desmoplakin and β-catenin, were also distributed normally at IDs (Fig. 2, d and h) in bitransgenic mice. In contrast, connexin-43, the main protein of gap junctions, was still localized laterally in these mice (Fig. 2 l), suggesting that its redistribution away from the ID in response to TNF-α signaling was independent of the desmin redistribution mechanism. These findings indicate that the cleavage of desmin is responsible for its removal from the IDs and that it mediates the subsequent disorganization of the ID architecture through the mislocalization of other ID proteins.

Desmin cleavage contributes to TNF-α–induced ubiquitin-positive aggregate formation

Our previous in vitro experiments suggest that the N-terminal product of desmin cleavage is completely unable to assemble into filaments and forms intracellular aggregates (Chen et al., 2003). We examined the presence of desmin aggregates and their possible colocalization with ubiquitin, a typical marker of aggresomes. We performed double immunolabeling on cryosections of MHCsTNF hearts for desmin and ubiquitin. Desmin immunostaining exhibited the typical Z-disk pattern but was also immunolocalized in aggregates that colocalized with ubiquitin (Fig. 8 A, b). The perinuclear accumulation distinguished the ubiquitin-desmin aggregates from the other cytoplasmic aggregates in which desmin colocalized with HSP25. It is known that the aggresomes are transported retrogradely on microtubules and accumulate in the perinuclear region (Garcia-Mata et al., 1999). At the age of 1 mo, the TNF-α–induced ubiquitin aggregates are more diffusely located in the cytoplasm, whereas at 3 mo, the aggregates seem to be more compact near the nucleus (Fig. 8 B, inset).

Ubiquitin aggregates in mice overexpressing TNF-α were decreased dramatically by ∼75% both in hearts lacking desmin as well as in hearts that coexpressed the D263E desmin (Fig. 8 B), suggesting that one of the major causes for the ubiquitin accumulation was related to the cleavage of desmin. Neither the WT nor the des$^{-/-}$ myocardium displayed any ubiquitin aggregates (not depicted). The remaining ubiquitin-positive aggregates in D263E MHCsTNF des$^{-/-}$ hearts do not colocalize with the caspase-resistant D263E desmin (Fig. 8 A, d–f). To further investigate the simultaneous presence of these ubiquitin-positive aggregates within polyubiquitinated proteins, we performed a Western blot analysis for ubiquitin. In the MHCsTNF mice, we detected an extensive laddering pattern that is characteristic of polyubiquitinated proteins, possibly as a result of reduced

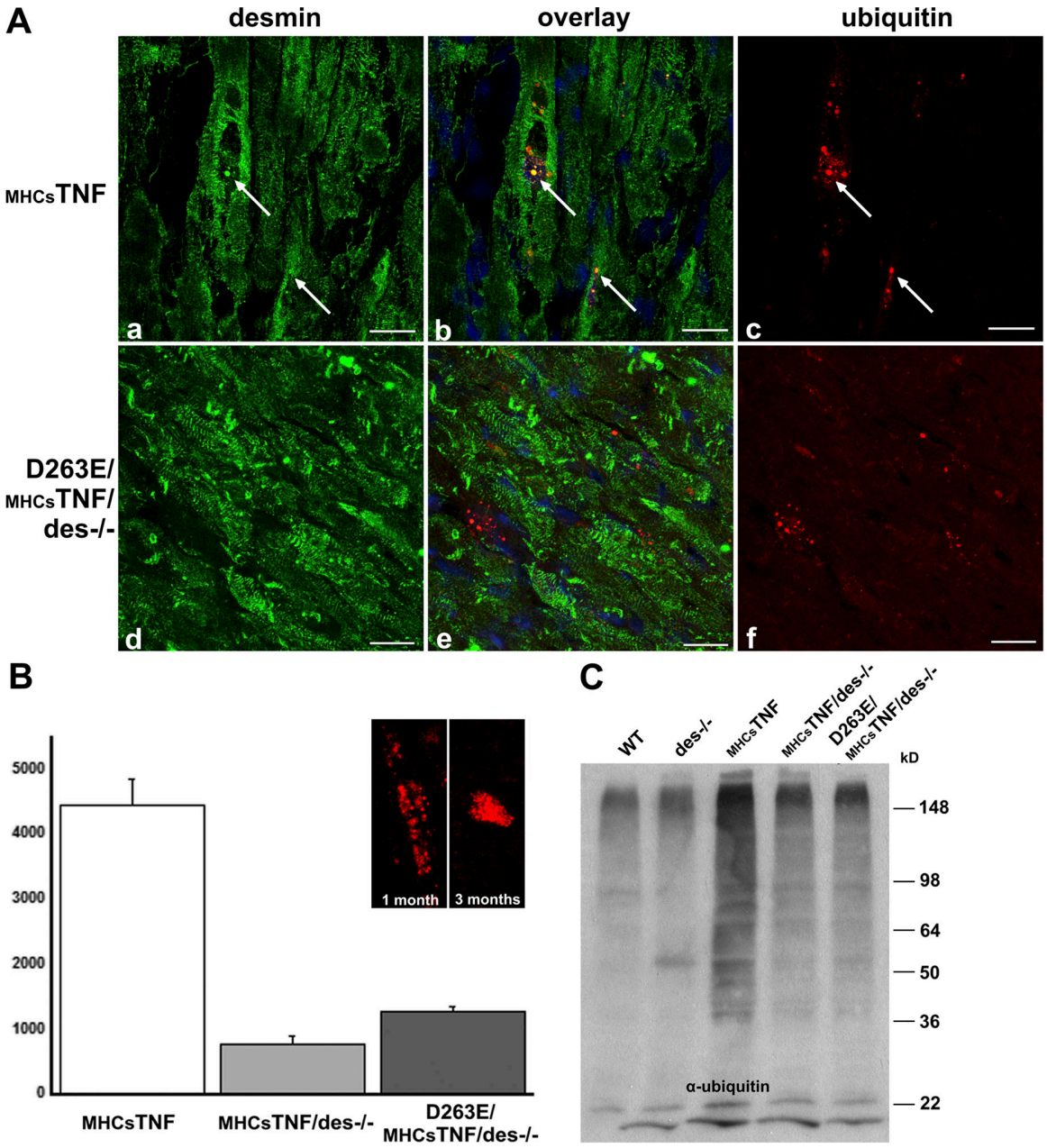

Figure 8. **The TNF-α–induced ubiquitin aggregates are decreased and do not colocalize with desmin in D263E MHCsTNF des$^{-/-}$ mice.** Cryosections from 3-mo-old MHCsTNF (a–c) and D263E MHCsTNF des$^{-/-}$ (d–f) mice were double immunolabeled for ubiquitin (c and f; red) and desmin (a and d; green). The arrows indicate ubiquitin aggregates that colocalize with desmin in MHCsTNF hearts. The field from the D263E MHCsTNF des$^{-/-}$ heart shown is not representative and was only selected to demonstrate the lack of colocalization with D263E desmin. (B) Quantification of the ubiquitin aggregates from 3-mo-old MHCsTNF, MHCsTNF des$^{-/-}$, and D263E MHCsTNF des$^{-/-}$ mice. These aggregates are diffused in the cytoplasm at the age of 1 mo and, in older mice, are compacted near the nucleus, as shown in the inset. Error bars represent SEM. (C) Ubiquitin levels in WT, des$^{-/-}$, MHCsTNF, MHCsTNF des$^{-/-}$, and D263E MHCsTNF des$^{-/-}$ 1-mo-old mice. Representative Western blot of the soluble fraction of these hearts. Bars, 20 µm.

proteasomal activity. This pattern was significantly reduced in MHCsTNF des$^{-/-}$ and D263E MHCsTNF des$^{-/-}$ mouse hearts (Fig. 8 C).

The presence of D263E desmin in the myocardium of D263E MHCsTNF des$^{-/-}$ mice attenuates apoptosis and improves cardiac function

We have shown that cardiomyocyte apoptosis contributes to LV wall thinning with the concomitant dilated phenotype (Engel et al., 2004; Haudek et al., 2007). We compared the prevalence of apoptotic cardiac nuclei in 3-mo-old MHCsTNF, MHCsTNF des$^{-/-}$, and D263E MHCsTNF des$^{-/-}$ mice to explore whether, apart from the stabilization of desmin and other proteins at IDs of D263E MHCsTNF des$^{-/-}$ hearts, the cardiomyocytes of these mice where more resistant to TNF-α–induced apoptotic stimuli. The prevalence of apoptosis was significantly reduced in MHCsTNF hearts (~75%) both in the absence of desmin as well as in mice harboring the D263E desmin (Fig. 9 A). However, the presence of the desmin mutant

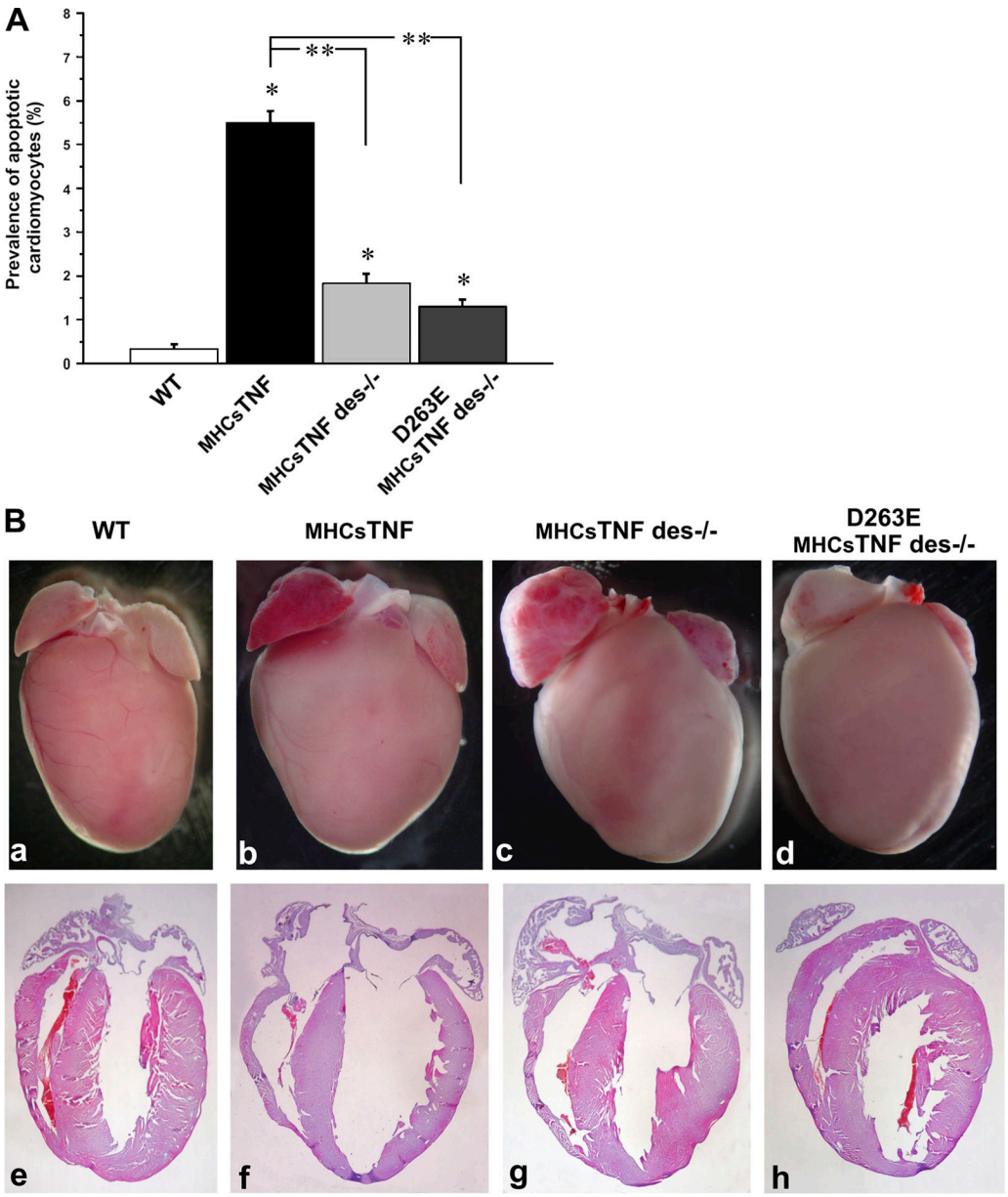

Figure 9. **Characterization of MHCsTNF des$^{-/-}$ and D263E MHCsTNF des$^{-/-}$ mice.** Measurement of apoptotic nuclei. (A) The percent prevalence of cardiomyocyte apoptosis was determined by in situ DNA ligation method in 3-mo-old WT, MHCsTNF, MHCsTNF des$^{-/-}$, and D263E MHCsTNF des$^{-/-}$ animals. *, $P < 0.05$ compared with WT; **, $P < 0.05$ between MHCsTNF and MHCsTNF des$^{-/-}$ or D263E MHCsTNF. Error bars represent SEM. (B) Gross morphology (a–d) and hematoxylin/eosin-stained paraffin sections (e–h) from 3-mo-old mice of the aforementioned categories.

did not completely abrogate cardiomyocyte apoptosis in D263E MHCsTNF des$^{-/-}$ mice because the prevalence of apoptosis was significantly greater than in WT hearts ($P < 0.001$).

Comparison of histological sections from the hearts of these mice reveals that the ventricular chambers of the D263E MHCsTNF des$^{-/-}$ mice are not dilated, and there is an increase of the myocardial thickness resembling the hypertrophic phenotype (Fig. 9 B, h), which could be the result of reduced apoptosis. On the other hand, to a lesser extent, the MHCsTNF des$^{-/-}$ hearts seem to delay the transition to dilated phenotype by preserving the thickness of the myocardium (Fig. 9 B, g).

To further explore the cardiac structure and function of the aforementioned genotypes of mice, we used standard morphometric analyses and 2D-directed M-mode echocardiography (Fig. 10 and Table S1, available at http://www.jcb.org/cgi/content/full/jcb.200710049/DC1). The LV end diastolic diameter (EDD), which is known to be considerably increased in 3-mo-old MHCsTNF mice compared with WT (Engel et al., 2004), was significantly lower in D263E MHCsTNF des$^{-/-}$ mice but still was increased compared with WT (Fig. 10 B). When we compared the LV posterior wall thickness (PWT), we found that in the D263E MHCsTNF des$^{-/-}$ mice, it was significantly increased compared with both MHCsTNF and WT. At this age, no difference caused by dilated wall thinning in the PWT of WT and MHCsTNF hearts was observed (Fig. 10 C). The decrease in LV EDD and the increase of PWT of the

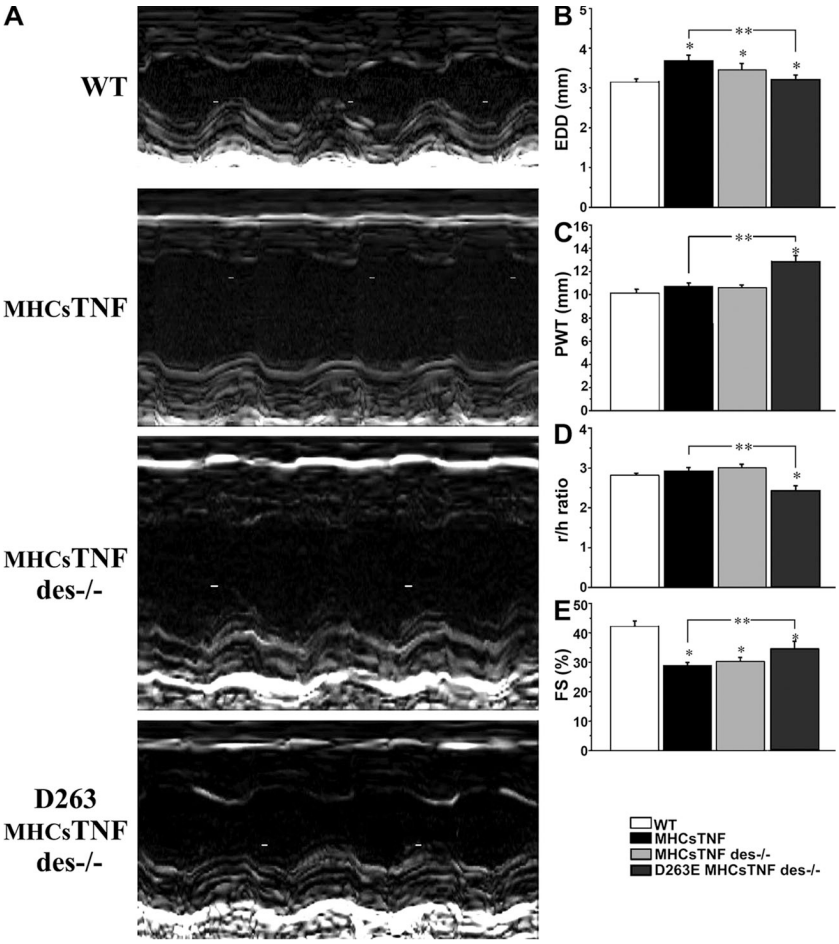

Figure 10. **Effect of D263E desmin on LV remodeling.** (A) Representative M-mode echocardiograms for WT, MHCsTNF, MHCsTNF des$^{-/-}$, and D263E MHCsTNF des$^{-/-}$ mouse hearts. (B–E) Group data for LV EDD (B), PWT (C), r/h (D), and percent FS (E) of the aforementioned mice categories. *, $P < 0.05$ compared with WT; **, $P < 0.05$ between MHCsTNF and/or D263E MHCsTNF. Error bars represent SEM.

D263E MHCsTNF des$^{-/-}$ hearts compared with MHCsTNF resulted in a significant decrease in the ratio of LV radius to LV wall thickness (r/h). This measurement suggests that the desmin mutant D263E prevented adverse cardiac remodeling in the MHCsTNF mice. Finally, the percentage of fractional shortening (FS) in D263E MHCsTNF des$^{-/-}$ mice increased significantly (21%) compared with MHCsTNF mice but did not reach WT levels. This was not only caused by LV EDD decrease but also by LV end systolic diameter improvement (Table S1). Thus, the caspase cleavage-resistant D263E desmin significantly inhibited the development of contractile dysfunction observed in MHCsTNF mice.

Discussion

Desmin is a target and mediator of TNF-α–induced alterations of ID components and heart failure development

TNF-α provokes cardiomyocyte apoptosis that contributes to the development of a heart failure phenotype through activation of both the extrinsic and intrinsic cell death pathways, with resultant activation of different members of the caspase family (Haudek et al., 2007). Disruption of the cytoskeleton is a key event in apoptotic pathways. There are several studies attempting to shed light on the role of the cleaved IF products in the execution of apoptosis without having unraveled, until now, the exact mechanism (for review see Oshima, 2002). The first important finding of this study is the loss of desmin and other junctional proteins from IDs in the heart of MHCsTNF mice. The localization of desmin at Z disks did not seem to be affected dramatically, thus suggesting a different and less dynamic association of desmin at these sites.

To study the involvement of desmin cleavage in the TNF-α–induced apoptotic pathways and its possible connection with its disappearance from IDs, we generated transgenic mice that express the caspase cleavage-resistant D263E desmin. In bitransgenic mice that overexpress both TNF-α and the D263E desmin, we observed that the latter remains localized at high levels at the IDs, indicating that desmin cleavage is a major step for its removal from IDs (Fig. 7 B). Here, we show for the first time that inhibition of TNF-α–induced cleavage of an IF rescues the proper maintenance of ID components at their position. Although the biological significance of such cleavage is not clearly known, it is widely accepted that it eliminates different protective mechanisms, thus facilitating cell death. The caspase-mediated proteolysis of the nuclear lamins may facilitate nuclear condensation, whereas cleavage of desmin might facilitate cardiomyocyte degeneration via mitochondrial collapse. As shown in Fig. 7 A, although the level of desmin cleavage in response to TNF-α was modest, the cleavage products of desmin were sufficient to cause IF aggregation. The caspase-mediated desmin degradation could act in parallel with other proteolytic enzymes, such as calpains,

which are known to be activated by TNF-α (Bajaj and Sharma, 2006) and could explain the other desmin fragment observed, specifically in TNF-α specimens (Fig. 7 A). This cleavage does not seem to contribute to the majority of the desmin aggregates and aggregate-related ID alterations, ameliorated extensively in D263E MHCsTNF des$^{-/-}$ mice, in which this fragment is still present. However, it could contribute to the remaining problems of these hearts.

We have shown that desmin cleavage mediates changes in the distribution of other proteins of the area composita such as desmoplakin, β-catenin (Fig. 2, d and h), and plakoglobin (not depicted). Desmin interacts directly through its C-terminal domain with desmoplakin (Lapouge et al., 2006), and deletions or missense mutations in the desmoplakin gene cause the loss of desmin from IDs (Kaplan et al., 2004; Yang et al., 2006). On the other hand, here we demonstrate that desmin is not required for the maintenance of desmoplakin at the IDs. Collectively, the aforementioned data show that desmoplakin is required for the anchorage of desmin to desmosomes; however, they do not explain why the modification of desmin is more crucial than its absence for desmoplakin destabilization. This is the first to report linking TNF-α signaling with the loss of desmin from IDs as well as the interference of desmin cleavage fragments with stabilization of other components of the IDs. However, the mechanism underlying this abnormal positioning of the ID proteins remains elusive.

TNF-α mediates cell–cell dissociation and is associated with the disordered expression of cadherin and β-catenin in endometrial epithelial cells (Tabibzadeh et al., 1995). Another study in primary cultures of human nasal and small airway epithelial cells has demonstrated that TNF-α induces the mislocalization of adhesion molecules such as E-cadherin and β-catenin, and it is involved in morphological change of the cells, with less coherence and rounder shape (Carayol et al., 2002). Our in vitro results are in accordance with our in vivo observations and confirm that TNF-α is a direct modulator of mislocalization of the ID proteins in cardiomyocytes (Fig. 3). These changes may result in a loss of the organization of IDs to a level that resembles immature ID formation during cardiac development (for review see Perriard et al., 2003), and it could be related, at least in part, to the cardiomyocyte disarray that predominates in the MHCsTNF myocardium.

One of the major structural alterations observed at the cardiomyocytes from patients with DCM involves the architecture and composition of the IDs, suggesting that one of the hallmarks of the disease might actually relate to changes in the contact sites between cardiomyocytes (for review see Perriard et al., 2003). Apart from desmoplakin, we examined the subcellular localization of β-catenin and connexin 43. β-Catenin shares a similar pattern to desmoplakin in the MHCsTNF myocytes because it loses its ID localization over time and is detected at the lateral side of the cells (Fig. 2). Colocalization experiments of desmoplakin and β-catenin revealed that the area composita of the IDs (as defined by Franke et al., 2006) in the MHCsTNF myocardium was uniformly affected and relocalizes from the bipolar ends of the rod-shaped cardiomyocytes to the lateral sarcolemma. The observation that the absence of desmin partially delayed the removal of these proteins from IDs and that these proteins largely retained their proper positioning with caspase-resistant D263E desmin suggests that TNF-α–induced desmin cleavage interferes with maintenance of the ID composition. However, the other ID proteins themselves could also be substrates for caspase cleavage or targets of other TNF-α–induced modifications because multiple proteolytic events regulate the dismantling of the cell–cell junctional complexes during apoptosis (Brancolini et al., 1998). These data could explain the quick disorganization of IDs in the primary culture of cardiomyocytes (Fig. 3). Connexin 43, the major ventricular myocyte connexin, seems to retain the mislocalization despite the preservation of the D263E desmin at IDs (Fig. 2 l). Sawaya et al. (2007) showed that in MHCsTNF mice, connexin 43 is dispersed away from the IDs without causing any decrease in ventricular myocyte conduction velocity or provoking ventricular arrhythmias. This is a very interesting finding considering that the IDs themselves in MHCsTNF cardiomyocytes, as shown in Fig. 1 B, are pretty disrupted.

Beyond desmin cleavage, another effect of the overexpression of TNF-α is desmin modification, most likely hyperphosphorylation. We propose that such modification of desmin could be the result of the apoptotic cascade starting by the overexpression of TNF-α. There are some reports correlating the hyperphosphorylation of IFs, including keratins and lamin B (Ku et al., 1997; Shimizu et al., 1998), with the collapse of cytoskeletal architecture during apoptosis. This hyperphosphorylation has been characterized as an early marker of apoptosis that has also been linked to cytoplasmic aggregates. However, it does not seem to be crucial for the final disorganization of the IF network but probably acts in a parallel process (Caulin et al., 1997; Ku et al., 1997; Schutte et al., 2004). As shown in Fig. 4, there is an increase in the number of acidic isoforms of desmin in MHCsTNF hearts that might correspond to the phosphorylated forms of desmin and might represent the nonfilamentous form of the protein (O'Connor et al., 1979). Phosphorylation-dependent disassembly of desmin filaments may facilitate its cleavage and contribute to sarcomere disarray in cardiomyocytes. The caspase-resistant D263E desmin not only inhibited the withdrawal of desmin and other ID proteins from the IDs of the bitransgenic hearts but also inhibited cardiomyocyte apoptosis (Fig. 9 A). Furthermore, it prevented LV wall thinning, adverse cardiac remodeling, and the decrease in FS that occurs in MHCsTNF mice (Fig. 10), strongly suggesting that desmin and potentially many other members of the scaffold it forms are major players in TNF-α–induced heart failure.

Desmin IFs as targets of TNF-α–induced aggregate formation and myocardial degeneration

Another important point of this study is the formation of desmin aggregates in MHCsTNF cardiomyocytes. Abnormal accumulation and aggregate formation of desmin within muscle cells was originally described as the morphological characteristic of DRM. Most of these disorders are caused by mutations in desmin or aberrant phosphorylation (Bar et al., 2004; Goldfarb et al., 2004; Schroder et al., 2007), whereas another form is associated with mutations in aB-crystallin, a chaperone protein known to associate with IFs (Vicart et al., 1998; Wang et al., 2001). These mutations result in the loss of desmin function and accumulation of mutant

misfolded desmin into insoluble toxic aggregates that gradually increase in the cytoplasm, attract other cytoskeletal-associated proteins, and eventually destroy the cell (Bar et al., 2004; Goldfarb et al., 2004; Schroder et al., 2007). Thus, desmin aggregates may exert toxic effects by sequestering away essential cellular proteins. Whether the accumulation of aggregates is more important to disease progression than the loss of desmin function remains to be resolved. In any case, these aggregates correlate with the IF-containing inclusion bodies of several degenerative diseases, including Alzheimer's and Parkinson's disease, amyotrophic lateral sclerosis, Alexander disease, and liver disease (for review see Zatloukal et al., 2007).

Desmin aggregates in the MHCsTNF cardiomyopathy model colocalize with HSP25, which has also been reported in desminopathies (Fischer et al., 2002). Absence of desmin in the MHCsTNF mouse hearts diminishes the intracellular aggregates of HSP25. Because the principal function of small HSP chaperones is to prevent the unfolding of cellular proteins damaged by stress, the accumulation of such chaperons in IF aggregates could be the result of an impaired chaperone unfolding activity.

There are contradictory data in the literature regarding the effect of TNF-α on HSP25. An in vitro study with murine L929 cells has reported that elevated levels of HSP25 can provide protection from TNF-α–induced cell death (Mehlen et al., 1996). On the other hand, it has been shown that HSP25 phosphorylation upon TNF-α stimulation down-regulates its chaperone capabilities by decreasing its oligomerization (Rogalla et al., 1999). Contrary to these in vitro data, in our in vivo model of TNF-α–induced cardiomyopathy, HSP25 showed an increase in an acidic isoform, which is probably the result of HSP25 phosphorylation by TNF-α as well as an additional, more alkaline isoform. The latter isoform appears to be correlated with desmin aggregation insofar as a previous study described that there is a shift of HSP27 to alkaline pH values in primary human desminopathies (Clemen et al., 2005).

Apart from the extensive desmin-positive aggregates that we found to colocalize with HSP25 (Fig. 5), there were also other aggregates of desmin that were more compact and tended to be restricted to a specific cell compartment that colocalized with ubiquitin in MHCsTNF mice (Fig. 8). We demonstrate in this study that the ubiquitin-positive aggregates are primarily caused by specific caspase cleavage of desmin at the 263 amino acid in response to TNF-α stimulus. There are two alternative hypotheses that could explain the accumulation of ubiquitin-positive aggregates. According to the first, above a threshold concentration, misfolded proteins globally impair proteasome activity (Bence et al., 2001). On the contrary, Bennett et al. (2005) have suggested that the impairment of the proteasomal activity occurs before coalescence of aggregated protein, which supports the hypothesis that sequestration of aggregates into inclusion bodies may be a protective rather than a pathogenic response (Kopito, 2000). Our data support the former hypothesis. The ultrastructural observations of this study (Fig. 1 B) demonstrate that the aggregates also contain cellular components such as vesicles, membranous whorls, and mitochondria that could represent the consequence of impaired proteosomal and/or autophagic activity. Furthermore, it is important to recognize that the aggregates may interfere with the sarcomere contraction and/or relaxation, thereby leading to impairment of cardiac function irrespective of the ubiquitin proteasome system (UPS). Indeed, this study demonstrates that myofibrillar alignment is disrupted by the presence of aggregates. Most importantly, particularly in the case of human desmin mutations, aggregate formation results in a loss of function, leading to mitochondrial problems resembling those initially observed in desmin-null mice (Milner et al., 2000; Schroder et al., 2003).

We have recently shown that in mice overexpressing TNF-α in the heart, there is a dysfunction of the UPS that is caused by decreased activity of the 26S proteasome (unpublished data). The present paper is the first study that interconnects the overexpression of TNF-α with ubiquitin-positive aggregates caused by accumulation of caspase-cleaved products. These aggregates may provoke a UPS dysfunction resulting in a cytoplasmic accumulation of polyubiquitinated proteins. Importantly, these polyubiquitinated conjugates were decreased in both the MHCsTNF des$^{-/-}$ and D263E MHCsTNF des$^{-/-}$ hearts (Fig. 8 C). It has been shown that transgenic expression of a deletion mutant desmin that lacks seven amino acids and has been identified in human patients with DRM forms extended aggregates that do lead to impairment of UPS function (Liu et al., 2006).

Our results suggest that like other degenerative diseases, cardiomyopathy may be associated with IF aggregate formation caused not only by a mutation in the corresponding IF gene but by other diverse abnormalities related to TNF-α or other signaling pathways. Importantly, our previous data have shown that overexpression of the antiapoptotic protein bcl-2 improved cardiac function both in the desmin-null and in the TNF-α–induced model of cardiomyopathy (Weisleder et al., 2004; Haudek et al., 2007). Thus, it is suggested that disturbance of the cytoskeleton–mitochodrial axis might be a major mechanism of heart failure development as well as other degenerative diseases, regardless of the original cause.

Materials and methods

Experimental animals

The Flag-tagged D263E mutant desmin construct was made as previously described (Chen et al., 2003). A 5.5-kb genomic fragment of the αMHC promoter was linked to Flag-D263E desmin. Isolated DNA was injected into C57BL/6J fertilized egg pronuclei using standard techniques to generate three transgenic lines. Mice lacking desmin (des$^{-/-}$) and mice overexpressing TNF-α (MHCsTNF) were generated as previously described (Milner et al., 1996; Li et al., 2000). MHCsTNF mice were backcrossed onto pure C57 mouse strain for five generations. Transgenic mice harboring either the D263E desmin or TNF-α were bred over two generations with des$^{-/-}$ mice to produce mice null for endogenous desmin (D263E des$^{-/-}$ and MHCsTNF des$^{-/-}$). Bitransgenic mice for D263E desmin and TNF-α (D263E MHCsTNF des$^{-/-}$) were produced from breeding of the two aforementioned mouse categories. All of the MHCsTNF mice studied were heterozygous. The procedures for the care and treatment of animals were performed according to institutional guidelines that follow those of the Association for Assessment and Accreditation of Laboratory Animal Care and the recommendations of the Federation of European Laboratory Animal Science Associations.

Primary culture of cardiomyocytes from neonatal rats

Hearts were harvested from 1–3-d-old neonatal rats, and, after removal of the atria, the ventricles were subjected to trypsin (Invitrogen) digestion in a final concentration of 100 μg/ml in HBSS for 16–18 h at 4°C. Further

collagenase digestion (type II collagenase; 150 U/ml; Worthington) was conducted at 37°C for 45 min. The mixture of cells was plated for 2 h in flasks to exclude fibroblasts. The remaining nonadherent cardiomyocytes were seeded on collagen-coated four-well chamber slides (Laboratory Tek) at a concentration of $1.5 \times 10^5/cm^2$. After 2 d, cells were incubated with 20 ng/ml TNF-α (recombinant murine TNF-α/TNFSF1A; R&D Systems) for different time points.

Immunofluorescence

10-µm cryosections and cells were fixed in 100% cold acetone for 20 min and 3 min, respectively, followed by blocking with 5% BSA in PBS for 1 h at RT. Primary antibodies including antidesmin (Santa Cruz Biotechnology, Inc.), antidesmoplakin (Serotec), anti–β-catenin (Sigma-Aldrich), anti-HSP25 (Assay Designs), anti–connexin 43 (Sigma-Aldrich), and antiubiquitin (Dako) were incubated with cryosections or cells for 3 h at RT. Samples were stained with AlexaFluor488 and 594 (Invitrogen) and mounted with fluorescent mounting medium (Dako). Images were taken at 23–24°C using an inverted laser-scanning confocal microscope (TCS SP5; Leica) equipped with a 63× NA 1.3 oil immersion objective lens (Leica) and LAS-AF acquisition software (Leica). Images were further processed (level adjustment) using Photoshop 7.0 (Adobe).

Immunoblotting

For heart crude extract preparation, mouse hearts were snap frozen in liquid nitrogen and homogenized in extraction buffer containing 10 mM Tris-HCl, pH 6.8, 1% Triton X-100, 1% SDS, 2 mM EDTA, and 1 mM DTT with protease inhibitor cocktail (Sigma-Aldrich). The homogenates were centrifuged for 10 min at 3,000 *g*. To distinguish the Triton X-100 soluble fraction from the pellet, the lysates (lysis buffer as above, without SDS) were clarified by centrifugation at 20,000 *g* for 30 min, and the Triton X-100 insoluble fractions were solubilized using the lysis buffer containing 9 M urea. Resolved proteins were transferred to polyvinylidene difluoride membranes (Bio-Rad Laboratories) and probed with antidesmin (Santa Cruz Biotechnology, Inc. and Sigma-Aldrich), anti-HSP25 (Stressgen; antiubiquitin (Chemicon), and anti-Flag (M2; Sigma-Aldrich). Secondary HRP-conjugated antibodies were purchased from Bio-Rad Laboratories.

2D gel electrophoresis

Hearts from WT and MHCsTNF were pulverized with liquid nitrogen and lyzed in lysis buffer (20 mM Tris-HCl containing 7 M urea, 2 M thiourea, 4% CHAPS, 10 mM 1,4-dithioerythritol, 1 mM EDTA, and protease and phosphatase inhibitors [0.2 mM Na_2VO_3 and 1 mM NaF]). The extracts were applied on immobilized pH 3–10 and pH 4–7 nonlinear gradient strip (Bio-Rad Laboratories) gel and separated overnight. Then, gels were equilibrated in SDS buffer, and the proteins were analyzed in the second dimension on 12% SDS-PAGE.

Echocardiography

Mice were anesthetized with an intraperitoneal injection of 100 mg/kg ketamine. Echocardiographic experiments were performed using an ultrasound system (Vivid 7; GE Healthcare) with a 13-MHz linear transducer. 2D targeted M-mode imaging was obtained from the short axis view at the level of greatest LV dimension. Images were analyzed using Echopac PC SW 3.1.3 software (GE Healthcare). Three beats were averaged for each measurement. The ratio of LV radius to PWT (r/h) and the percentage of LV FS (FS [%] = [(EDD − ESD)/EDD] × 100) were calculated.

Cardiomyocyte apoptosis

Apoptotic cardiomyocytes were identified using the In Situ Cell Death Detection kit (Roche) according to the manufacturer's instructions on paraffin-embedded myocardial sections from 3-mo-old mouse hearts. To distinguish cardiomyocytes from nonmuscle cells, the myocardial sections were previously labeled with anti–α-actinin (Sigma-Aldrich).

Electron microscopy

Samples from two WT and MHCsTNF mice were processed for transmission electron microscopy as previously described (Milner et al., 2000). In brief, hearts were perfused with cold 2.5% gluteraldehyde, and dissected ventricles were sliced into 1-mm cubes and fixed for 16 h at 4°C in the same fixative followed by postfixation in 1% osmium tetroxide for 2 h at room temperature. Samples were then dehydrated through an ethanol series and passed into Embed 812 (EMS) by using propylene oxide as a transitional solvent. Embedded blocks were cured at 65°C for 48 h and sectioned at 80 nm.

Statistics

Data were expressed as mean ± SEM. Statistical comparisons were performed using analysis of variance with Student-Newman-Kuels post-hoc test or the unpaired *t* test where appropriate. A p-value of <0.05 was considered statistically significant.

Online supplemental material

Fig. S1 shows the subcellular localization of desmin, desmoplakin, β-catenin, and connexin 43 in MHCsTNF and WT myocardium at the age of 15 d after birth. Fig. S2 shows the localization of desmoplakin, β-catenin, and connexin 43 in WT, $des^{-/-}$ and D263E $des^{-/-}$ hearts at the age of 3 mo. Table S1 presents the parameters from the echocardiographic analysis. Online supplemental material is available at http://www.jcb.org/cgi/content/full/jcb.200710049/DC1.

We thank Dr. S. Pagkakis and Dr. E. Rigana for their help with confocal imaging. We are grateful to Prof. J. D'hooge and S. Tombeur (University Hospital Gasthuisberg, Cardiovascular Imaging and Dynamics Laboratory, Leuven, Belgium) and K. Picassetos (GE Medical) for their help on mice echocardiography.

This work was supported by the Biomedical Research Foundation of the Academy of Athens, by funds from the Greek Secretariat of Research and Development (grants PENED 01ED371/Onassio Cardiac Surgery Center and PEP ATT_39) to Y. Capetanaki, and by funds from the National Institutes of Health (grants P50 HL-O6H, RO1 HL58081, and RO1 HL73017) to D.L. Mann.

Submitted: 8 October 2007
Accepted: 1 May 2008

References

Bajaj, G., and R.K. Sharma. 2006. TNF-alpha-mediated cardiomyocyte apoptosis involves caspase-12 and calpain. *Biochem. Biophys. Res. Commun.* 345:1558–1564.

Bar, H., S.V. Strelkov, G. Sjoberg, U. Aebi, and H. Herrmann. 2004. The biology of desmin filaments: how do mutations affect their structure, assembly, and organisation? *J. Struct. Biol.* 148:137–152.

Bence, N.F., R.M. Sampat, and R.R. Kopito. 2001. Impairment of the ubiquitin-proteasome system by protein aggregation. *Science.* 292:1552–1555.

Bennett, E.J., N.F. Bence, R. Jayakumar, and R.R. Kopito. 2005. Global impairment of the ubiquitin-proteasome system by nuclear or cytoplasmic protein aggregates precedes inclusion body formation. *Mol. Cell.* 17:351–365.

Brancolini, C., A. Sgorbissa, and C. Schneider. 1998. Proteolytic processing of the adherens junctions components beta-catenin and gamma-catenin/plakoglobin during apoptosis. *Cell Death Differ.* 5:1042–1050.

Byun, Y., F. Chen, R. Chang, M. Trivedi, K.J. Green, and V.L. Cryns. 2001. Caspase cleavage of vimentin disrupts intermediate filaments and promotes apoptosis. *Cell Death Differ.* 8:443–450.

Capetanaki, Y., D.J. Milner, and G. Weitzer. 1997. Desmin in muscle formation and maintenance: knockouts and consequences. *Cell Struct. Funct.* 22:103–116.

Capetanaki, Y., R.J. Bloch, A. Kouloumenta, M. Mavroidis, and S. Psarras. 2007. Muscle intermediate filaments and their links to membranes and membranous organelles. *Exp. Cell Res.* 313:2063–2076.

Carayol, N., A. Campbell, I. Vachier, B. Mainprice, J. Bousquet, P. Godard, and P. Chanez. 2002. Modulation of cadherin and catenins expression by tumor necrosis factor-alpha and dexamethasone in human bronchial epithelial cells. *Am. J. Respir. Cell Mol. Biol.* 26:341–347.

Caulin, C., G.S. Salvesen, and R.G. Oshima. 1997. Caspase cleavage of keratin 18 and reorganization of intermediate filaments during epithelial cell apoptosis. *J. Cell Biol.* 138:1379–1394.

Chen, F., R. Chang, M. Trivedi, Y. Capetanaki, and V.L. Cryns. 2003. Caspase proteolysis of desmin produces a dominant-negative inhibitor of intermediate filaments and promotes apoptosis. *J. Biol. Chem.* 278:6848–6853.

Clemen, C.S., D. Fischer, U. Roth, S. Simon, P. Vicart, K. Kato, A.M. Kaminska, M. Vorgerd, L.G. Goldfarb, B. Eymard, et al. 2005. Hsp27-2D-gel electrophoresis is a diagnostic tool to differentiate primary desminopathies from myofibrillar myopathies. *FEBS Lett.* 579:3777–3782.

Engel, D., R. Peshock, R.C. Armstong, N. Sivasubramanian, and D.L. Mann. 2004. Cardiac myocyte apoptosis provokes adverse cardiac remodeling in transgenic mice with targeted TNF overexpression. *Am. J. Physiol. Heart Circ. Physiol.* 287:H1303–H1311.

Feldman, A.M., A. Combes, D. Wagner, T. Kadakomi, T. Kubota, Y.Y. Li, and C. McTiernan. 2000. The role of tumor necrosis factor in the pathophysiology of heart failure. *J. Am. Coll. Cardiol.* 35:537–544.

Fischer, D., J. Matten, J. Reimann, C. Bonnemann, and R. Schroder. 2002. Expression, localization and functional divergence of alphaB-crystallin and heat shock protein 27 in core myopathies and neurogenic atrophy. *Acta Neuropathol.* 104:297–304.

Franke, W.W., C.M. Borrmann, C. Grund, and S. Pieperhoff. 2006. The area composita of adhering junctions connecting heart muscle cells of vertebrates. I. Molecular definition in intercalated disks of cardiomyocytes by immunoelectron microscopy of desmosomal proteins. *Eur. J. Cell Biol.* 85:69–82.

Garcia-Mata, R., Z. Bebok, E.J. Sorscher, and E.S. Sztul. 1999. Characterization and dynamics of aggresome formation by a cytosolic GFP-chimera. *J. Cell Biol.* 146:1239–1254.

Goldfarb, L.G., P. Vicart, H.H. Goebel, and M.C. Dalakas. 2004. Desmin myopathy. *Brain.* 127:723–734.

Haudek, S.B., G.E. Taffet, M.D. Schneider, and D.L. Mann. 2007. TNF provokes cardiomyocyte apoptosis and cardiac remodeling through activation of multiple cell death pathways. *J. Clin. Invest.* 117:2692–2701.

Kaplan, S.R., J.J. Gard, L. Carvajal-Huerta, J.C. Ruiz-Cabezas, G. Thiene, and J.E. Saffitz. 2004. Structural and molecular pathology of the heart in Carvajal syndrome. *Cardiovasc. Pathol.* 13:26–32.

Kayalar, C., T. Ord, M.P. Testa, L.T. Zhong, and D.E. Bredesen. 1996. Cleavage of actin by interleukin 1 beta-converting enzyme to reverse DNase I inhibition. *Proc. Natl. Acad. Sci. USA.* 93:2234–2238.

Kopito, R.R. 2000. Aggresomes, inclusion bodies and protein aggregation. *Trends Cell Biol.* 10:524–530.

Ku, N.O., J. Liao, and M.B. Omary. 1997. Apoptosis generates stable fragments of human type I keratins. *J. Biol. Chem.* 272:33197–33203.

Lapouge, K., L. Fontao, M.F. Champliaud, F. Jaunin, M.A. Frias, B. Favre, D. Paulin, K.J. Green, and L. Borradori. 2006. New insights into the molecular basis of desmoplakin- and desmin-related cardiomyopathies. *J. Cell Sci.* 119:4974–4985.

Latini, R., M. Bianchi, E. Correale, C.A. Dinarello, G. Fantuzzi, C. Fresco, A.P. Maggioni, M. Mengozzi, S. Romano, L. Shapiro, et al. 1994. Cytokines in acute myocardial infarction: selective increase in circulating tumor necrosis factor, its soluble receptor, and interleukin-1 receptor antagonist. *J. Cardiovasc. Pharmacol.* 23:1–6.

Lazebnik, Y.A., A. Takahashi, R.D. Moir, R.D. Goldman, G.G. Poirier, S.H. Kaufmann, and W.C. Earnshaw. 1995. Studies of the lamin proteinase reveal multiple parallel biochemical pathways during apoptotic execution. *Proc. Natl. Acad. Sci. USA.* 92:9042–9046.

Li, X., M.R. Moody, D. Engel, S. Walker, F.J. Clubb Jr., N. Sivasubramanian, D.L. Mann, and M.B. Reid. 2000. Cardiac-specific overexpression of tumor necrosis factor-alpha causes oxidative stress and contractile dysfunction in mouse diaphragm. *Circulation.* 102:1690–1696.

Li, Y.Y., D. Chen, S.C. Watkins, and A.M. Feldman. 2001. Mitochondrial abnormalities in tumor necrosis factor-alpha-induced heart failure are associated with impaired DNA repair activity. *Circulation.* 104:2492–2497.

Li, Z., E. Colucci-Guyon, M. Pincon-Raymond, M. Mericskay, S. Pournin, D. Paulin, and C. Babinet. 1996. Cardiovascular lesions and skeletal myopathy in mice lacking desmin. *Dev. Biol.* 175:362–366.

Liu, J., Q. Chen, W. Huang, K.M. Horak, H. Zheng, R. Mestril, and X. Wang. 2006. Impairment of the ubiquitin-proteasome system in desminopathy mouse hearts. *FASEB J.* 20:362–364.

Mann, D.L. 2003. Stress-activated cytokines and the heart: from adaptation to maladaptation. *Annu. Rev. Physiol.* 65:81–101.

Mehlen, P., C. Kretz-Remy, X. Preville, and A.P. Arrigo. 1996. Human hsp27, *Drosophila* hsp27 and human alphaB-crystallin expression-mediated increase in glutathione is essential for the protective activity of these proteins against TNFalpha-induced cell death. *EMBO J.* 15:2695–2706.

Milner, D.J., G. Weitzer, D. Tran, A. Bradley, and Y. Capetanaki. 1996. Disruption of muscle architecture and myocardial degeneration in mice lacking desmin. *J. Cell Biol.* 134:1255–1270.

Milner, D.J., M. Mavroidis, N. Weisleder, and Y. Capetanaki. 2000. Desmin cytoskeleton linked to muscle mitochondrial distribution and respiratory function. *J. Cell Biol.* 150:1283–1298.

O'Connor, C.M., D.R. Balzer Jr., and E. Lazarides. 1979. Phosphorylation of subunit proteins of intermediate filaments from chicken muscle and nonmuscle cells. *Proc. Natl. Acad. Sci. USA.* 76:819–823.

Oshima, R.G. 2002. Apoptosis and keratin intermediate filaments. *Cell Death Differ.* 9:486–492.

Perriard, J.C., A. Hirschy, and E. Ehler. 2003. Dilated cardiomyopathy: a disease of the intercalated disc? *Trends Cardiovasc. Med.* 13:30–38.

Rogalla, T., M. Ehrnsperger, X. Preville, A. Kotlyarov, G. Lutsch, C. Ducasse, C. Paul, M. Wieske, A.P. Arrigo, J. Buchner, and M. Gaestel. 1999. Regulation of Hsp27 oligomerization, chaperone function, and protective activity against oxidative stress/tumor necrosis factor alpha by phosphorylation. *J. Biol. Chem.* 274:18947–18956.

Sawaya, S.E., Y.S. Rajawat, T.G. Rami, G. Szalai, R.L. Price, N. Sivasubramanian, D.L. Mann, and D.S. Khoury. 2007. Downregulation of connexin40 and increased prevalence of atrial arrhythmias in transgenic mice with cardiac-restricted overexpression of tumor necrosis factor. *Am. J. Physiol. Heart Circ. Physiol.* 292:H1561–H1567.

Schröder, R., B. Goudeau, M.C. Simon, D. Fischer, T. Eggermann, C.S. Clemen, Z. Li, J. Reimann, Z. Xue, S. Rudnik-Schöneborn, et al. 2003. On noxious desmin: functional effects of a novel heterozygous desmin insertion mutation on the extrasarcomeric desmin cytoskeleton and mitochondria. *Hum. Mol. Genet.* 12:657–669.

Schröder, R., A. Vrabie, and H.H. Goebel. 2007. Primary desminopathies. *J. Cell. Mol. Med.* 11:416–426.

Schutte, B., M. Henfling, W. Kolgen, M. Bouman, S. Meex, M.P. Leers, M. Nap, V. Bjorklund, P. Bjorklund, B. Bjorklund, et al. 2004. Keratin 8/18 breakdown and reorganization during apoptosis. *Exp. Cell Res.* 297:11–26.

Seidman, J.G., and C. Seidman. 2001. The genetic basis for cardiomyopathy: from mutation identification to mechanistic paradigms. *Cell.* 104:557–567.

Shimizu, T., C.X. Cao, R.G. Shao, and Y. Pommier. 1998. Lamin B phosphorylation by protein kinase calpha and proteolysis during apoptosis in human leukemia HL60 cells. *J. Biol. Chem.* 273:8669–8674.

Sivasubramanian, N., M.L. Coker, K.M. Kurrelmeyer, W.R. MacLellan, F.J. DeMayo, F.G. Spinale, and D.L. Mann. 2001. Left ventricular remodeling in transgenic mice with cardiac restricted overexpression of tumor necrosis factor. *Circulation.* 104:826–831.

Tabibzadeh, S., Q.F. Kong, S. Kapur, P.G. Satyaswaroop, and K. Aktories. 1995. Tumour necrosis factor-alpha-mediated dyscohesion of epithelial cells is associated with disordered expression of cadherin/beta-catenin and disassembly of actin filaments. *Hum. Reprod.* 10:994–1004.

Thornell, L., L. Carlsson, Z. Li, M. Mericskay, and D. Paulin. 1997. Null mutation in the desmin gene gives rise to a cardiomyopathy. *J. Mol. Cell. Cardiol.* 29:2107–2124.

Torre-Amione, G., S. Kapadia, J. Lee, J.B. Durand, R.D. Bies, J.B. Young, and D.L. Mann. 1996. Tumor necrosis factor-alpha and tumor necrosis factor receptors in the failing human heart. *Circulation.* 93:704–711.

Towbin, J.A., and N.E. Bowles. 2002. The failing heart. *Nature*. 415:227–233.

Vicart, P., A. Caron, P. Guicheney, Z. Li, M.C. Prevost, A. Faure, D. Chateau, F. Chapon, F. Tome, J.M. Dupret, et al. 1998. A missense mutation in the alphaB-crystallin chaperone gene causes a desmin-related myopathy. *Nat. Genet.* 20:92–95.

Wang, X., H. Osinska, R. Klevitsky, A.M. Gerdes, M. Nieman, J. Lorenz, T. Hewett, and J. Robbins. 2001. Expression of R120G-alphaB-crystallin causes aberrant desmin and alphaB-crystallin aggregation and cardiomyopathy in mice. *Circ. Res.* 89:84–91.

Weisleder, N., G.E. Taffet, and Y. Capetanaki. 2004. Bcl-2 overexpression corrects mitochondrial defects and ameliorates inherited desmin null cardiomyopathy. *Proc. Natl. Acad. Sci. USA.* 101:769–774.

Yang, Z., N.E. Bowles, S.E. Scherer, M.D. Taylor, D.L. Kearney, S. Ge, V.V. Nadvoretskiy, G. DeFreitas, B. Carabello, L.I. Brandon, et al. 2006. Desmosomal dysfunction due to mutations in desmoplakin causes arrhythmogenic right ventricular dysplasia/cardiomyopathy. *Circ. Res.* 99:646–655.

Zatloukal, K., S.W. French, C. Stumptner, P. Strnad, M. Harada, D.M. Toivola, M. Cadrin, and M.B. Omary. 2007. From Mallory to Mallory-Denk bodies: what, how and why? *Exp. Cell Res.* 313:2033–2049.